

Ordering, Graphoepitaxial Orientation, and Conformation of a Polyfluorene Derivative of the “Hairy-Rod” Type on an Oriented Substrate of Polyimide[†]

Günter Lieser,* Masao Oda,[‡] Tzenka Miteva, Andreas Meisel, Heinz-Georg Nothofer, and Ullrich Scherf

Max-Planck-Institut für Polymerforschung, Ackermannweg 10, D-55128 Mainz, Germany

Dieter Neher

Universität Potsdam, Institut für Physik, Am Neuen Palais 10, D-14469 Potsdam, Germany; and Max-Planck-Institut für Polymerforschung, Ackermannweg 10, D-55128 Mainz, Germany

Received December 28, 1999; Revised Manuscript Received March 30, 2000

ABSTRACT: Spin-coated films of an ethylhexyl derivative of polyfluorene can be converted on a pretreated polyimide substrate into highly oriented films by annealing in the liquid crystalline state. Together with improving orientation segregation of the wormlike molecules with respect to chain lengths and lamella formation proceeds. End groups are preferentially assembled in interlamellar regions. This morphological feature is thought to influence all measurements of intrinsic properties of polyfluorene films with similar histories. Electron diffraction patterns of the film are identical with X-ray fiber diagrams of fibers drawn from the melt and annealed in the liquid crystalline state. The experimental data show that the polymer molecules adopt a helical (5/2) conformation, packing in a trigonal unit cell. Molecular modeling based on ab initio MO calculations have been carried out to obtain independent estimates of chain geometry and conformation. These calculations are more in favor of a 5/2 rather than a 5/1 helix, with the argument of the observed packing of the individual PF chains and a plausibly low torsion angle of adjacent fluorene building blocks only for a 5/2 helix.

Introduction

Polyfluorenes **PF** have involved as an important class of materials for polymer light-emitting diodes (LED). Several reports have demonstrated bright blue emission from PF homo- and copolymers.¹ Color tuning was achieved via copolymerization with benzothiadiazole or anthracene.² A second important property of **PF** homopolymers is their thermotropic liquid-crystallinity, which allows to orient these polymers on rubbed polyimide layers.³ By doping of the polyimide layer with appropriate hole-transporting molecules, polarized LEDs with a state-of-the-art dichroic ratio in emission of more than 20 and a brightness in excess of 100 Cd/m² could be fabricated.⁴

Many questions concerning the backbone structure and the morphology of the **PF** emission layers need, however, still to be elucidated. In a recent paper Grell et al. demonstrated⁵ that a strong correlation exists between the optical properties in absorption and the main chain order. Depending on preparation conditions, the conjugation was limited either by chain disorder or due to the intrinsic electronic structure of the nondisturbed **PF** chain. A particular feature of the ordered state was the appearance of a sharp absorption peak at 437 nm. Further, a planar zigzag conformation was suggested for the well-ordered state.

A second observation is that the maximum alignment in thin solid films depends on the nature of the side chains. While the dichroic ratio in absorption barely

exceeds 10 for poly(9,9-bis(*n*-octyl)fluorene-2,7-diyl) (**PFO**) with linear octyl side chains, values larger than 15 are achievable in the case of poly(9,9-bis(2-ethylhexyl)fluorene-2,7-diyl) (**PF2/6**, Scheme 1). In the latter case, the characteristic absorption band of the highly ordered state is missing even after prolonged annealing in the LC phase.

This paper reports on the analysis of thin oriented layers of **PF2/6** by electron microscopy and diffraction. It is shown that these films are polycrystalline at room temperature. The investigations reveal a highly ordered hexagonal packing of individual **PF** chains with a helical backbone conformation. These findings are supported by molecular modeling based on ab initio MO calculations, which suggest that only the helical or the planar zigzag conformation yield linear polyfluorene chains. The calculations indicate further that, for our **PF2/6** macromolecules and neglecting interchain interactions, the helix conformation is energetically favored.

Experimental and Calculation Method

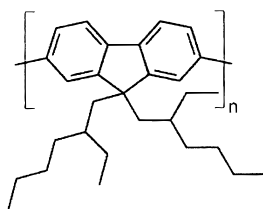
Synthesis of polyfluorene (**PF2/6**) and preparation of the oriented polyimide (PI) layer are described elsewhere.^{3a} The **PF2/6** used here has PS equivalent molecular weights $M_n = 147\,000$ and $M_w = 262\,000$. A solution-cast sample of this polymer shows melting into a liquid crystalline phase at 169 °C. The films of **PF2/6** were spin-coated from a 10 g/L solution in toluene onto the pretreated PI substrates. After evaporation of the solvent the films were annealed at 175 °C for 2 h in inert atmosphere and cooled to room temperature at a rate of about 3 K/min. The final thickness of the PI alignment layer was 30 nm and of the **PF2/6** was 20 nm as measured by a Tencor α -step profiler.

In the optical microscope between crossed polarizers a complete extinction all over the films was observed to appear at every 90° stage rotation interval, when the PI orientation

[†] Dedicated to Professor Gerhard Wegner on the occasion of his 60th birthday.

[‡] Current address: Universität Potsdam, Institut für Physik, Am Neuen Palais 10, D-14469 Potsdam, Germany.

Scheme 1



direction in the samples was exactly parallel to one of the polarizers.^{3b} This reveals a high orientation of the **PF2/6** films.

For the sake of electron microscopical observation the film and the polyimide substrate were floated off the supporting glass slide onto a water surface and transferred to 600 mesh copper grids. The film was examined in a LEO 912 transmission electron microscope (TEM) without carbon supporting film. The electron energy loss (EEL) spectrometer, integrated in the column of the TEM, was used to suppress inelastic scattering of energy losses exceeding 20 eV in the case of electron diffraction and elastic darkfield imaging. Some micrographs were taken to record mass thickness distribution at an energy loss of 100 eV for comparison with the elastic dark field micrographs. Electron diffraction patterns were recorded on photographic Ilford PAN F film and calibrated with TiCl_3 powder. The diffraction patterns were evaluated after 10-fold magnification in a darkroom magnifier.

In addition, fibers were drawn from a liquid crystalline **PF2/6** melt (175 °C) and annealed at 175 °C for 4 and 24 h. X-ray fiber diagrams were recorded in a vacuum flat film camera (Huber, Germany).

Molecular orbital calculations were carried out using the Gaussian 98 program on a DEC 2100 4/266 workstation at the Max-Planck-Institut für Polymerforschung. Structural optimizations of bi- and terfluorene were carried out by the RHF method with 6-31G and 6-31G(d,p) (d type diffuse function on C, and p type diffuse function on H) basis set. The torsional angle dependence of the S_0-S_1 transition energy of bifluorene was calculated by time dependent (TD) methods (random phase approximation (RPA)) at Hartree-Fock level within the Gaussian 98 program. For each angle, the structure was optimized prior to the calculation of the transition energy.

Results and Discussion

Electron- and X-ray diffraction. According to preliminary studies of **PF2/6** films in an polarizing microscope one could expect that they would exhibit high orientation when investigated by means of electron diffraction. Figure 1. displays a typical electron diffraction pattern from a circular area of 2.7 μm in diameter indicating that the film texture is fiberlike. The interpretation of the fiber diagram will be postponed at the moment and we switch first over to the morphology of the film. TEM brightfield micrographs do not exhibit morphological features at all although they are present as evidenced best in an elastic darkfield image taken in the light of the meridional reflection. Such a darkfield micrograph is displayed in Figure 2a. Over the whole area bright bands are seen interrupted by black stripes in a preferential direction perpendicular to the rubbing direction of the **PI** substrate. The lateral extension of the band-like domains exceeds the bandwidth between the stripes by far.

The micrograph can be interpreted along phenomena which are common to hairy rod molecules.⁶⁻⁹ In analogy to electron micrographs of stained ultrathin sections of partially crystallized polymers we use the picture of lamellae separated by disordered areas also for the hairy rod molecules. These lamellae are seen in the current case edge-on. In a thin film with chain orientation parallel to the substrate the lamellae are reduced to the



Figure 1. Electron diffraction pattern of **PF2/6** oriented on top of polyimide from a circular area of 2.7 μm in diameter (meridian in direction SW-NE). (The visible asymmetry of the reflection intensities on the fifth layer line is due to a small deviation from the normal beam incidence, probably due to an immanent slight curvature of the film inside the mesh of the supporting grid.)

bands seen in the microscope. During annealing the hairy rod polymers are in an anisotropic melt and adopt parallel orientation. With increasing dwell time in the liquid crystalline state lamellae are formed in a first stage. Inside the lamellae the chains are oriented more or less perpendicular to the stripes (perpendicular to the lamella surface). The lamella thickness is strongly correlated to the number-average of the chain length,⁶ but owing to the chain length (molecular weight) distribution, the lamella surface is rough. In a later stage of the liquid crystalline state, the molecules inside the lamellar domains segregate with respect to their lengths; the lamellae get wedge shaped, having expelled the shorter chains toward the lamella ends. Sometimes an alternating sequence of thick and thin lamellae is observed.

In the hitherto investigated lyotropic and thermotropic systems, the demixing of chains was connected to annihilation of disclinations in the director fields of the liquid crystals. In the current example of **PF2/6** the oriented substrate prevents the formation of similar singularities or accelerates their annihilation. The unique orientation over large areas is favored by "graphoepitaxy", an expression introduced by Flanders et al. at the example of oriented growth of silicon on artificial surface patterns in amorphous substrates.¹⁰

The current micrograph of Figure 2a shows **PF2/6**-lamellae formed in the liquid crystalline state and fixed by the subsequent crystallization during cooling to the ambient. The segregation of chains with respect to their lengths has proceeded into the second stage reflecting already the molecular weight distribution by the non-uniform lamella thickness. The lamellae contain in their thicker parts **PF2/6** chains of a degree of polymerization (DP) of ~ 300 and correspond in their wedge shaped ends to molecules of $\text{DPs} \leq 100$ in agreement to molecular weight measurements. The tiny stripes are small fis-

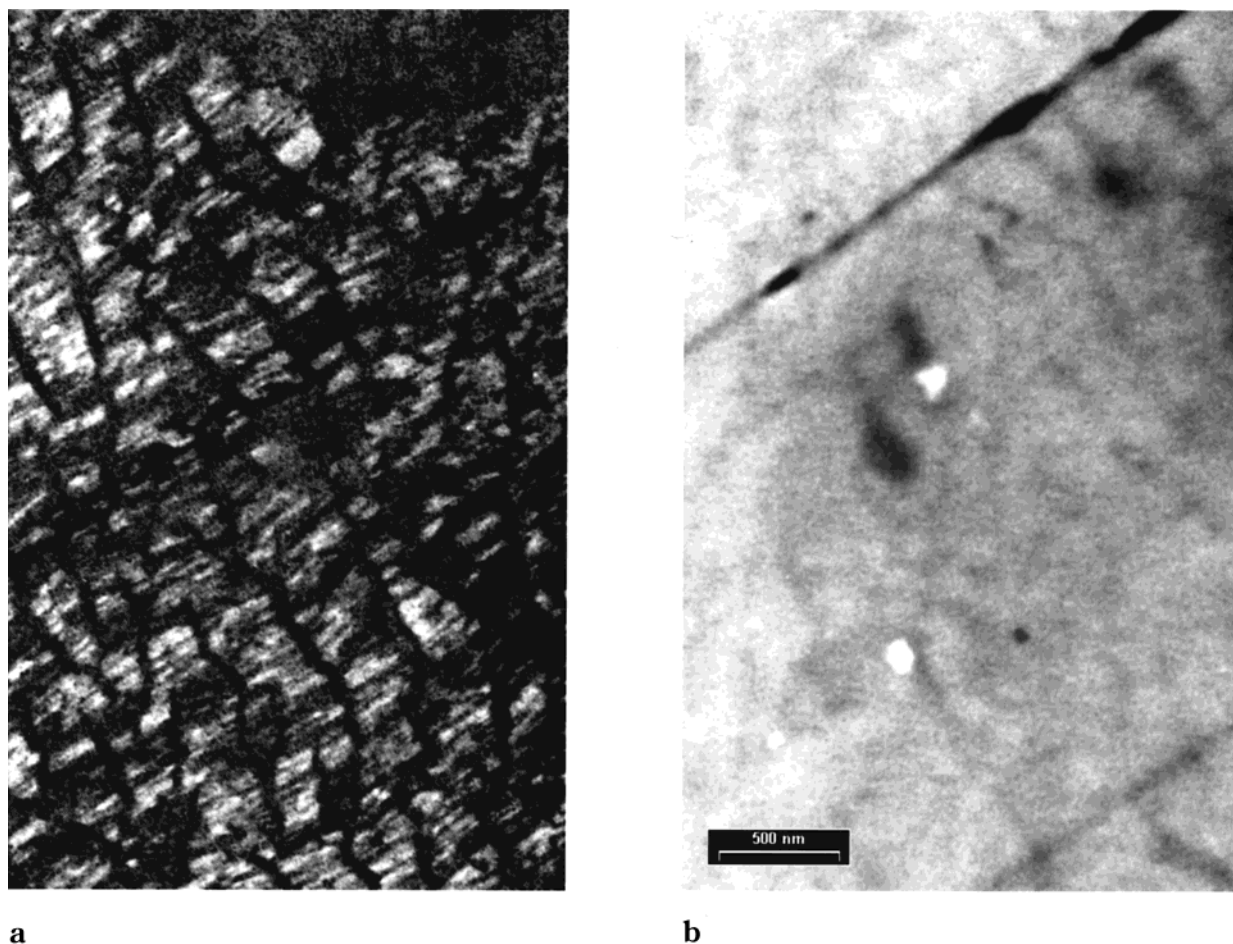


Figure 2. Electron micrographs of an oriented PF2/6 film: (a) dark field image in the light of the 00.5 reflection; (b) mass thickness distribution in the same area by an inelastic darkfield image at an electron energy loss of 100 eV.

tures presumably formed during cooling to room temperature by an increase of density in tight contact to the PI substrate. They indicate the molecular direction. The micrograph shows narrow areas between the lamellae wherein the end groups of the main chains are concentrated. The end groups and residual disorder owing to the chain length distribution prevent the formation of crystalline order in the interlamellar regions. They are therefore imaged in the darkfield as black lines predominantly perpendicular to the molecular direction.

Even so, the film does not become discontinuous by the interlamellar regions because there are also much longer chains running through the interlamellar regions, the number of which is a function of the current type of molecular weight distribution. In the case of a (here unfounded) normal distribution, 37% of the molecules are longer than the number-average and 14% are longer than twice the average chain length.

The disturbed interlamellar regions are thought to give rise to some properties of the film not being intrinsic for the material. So the path to prepare an oriented film is ambiguous. On one hand, the orientation in the liquid crystalline state is rather efficient, at the other hand the continuity of the film is disturbed by segregation of the chains with respect to their lengths. The effect demonstrated clearly by elastic dark field image is nearly overseen by conventional electron microscopy. Electron microscopy with inelastic scattered electrons is able to verify that the continuity of the film is disturbed but the film does not become disrupted by

the interlamellar areas. Figure 2b displays the same area as Figure 2a, but in inelastic darkfield at an electron energy loss of 100 eV. By this technique, the mass thickness distribution of the film is emphasized. One sees a few lines being slightly darker than the image on the average which coincide with black lines in the elastic dark field image Figure 2a. At the curved dark lines the film thickness is slightly reduced with respect to the average film thickness. Their preferential direction is perpendicular to the rubbing direction of the polyimide substrate and varying owing to the chain length distribution. The molecular director, however, adopts the orientation of the underlying scratches produced by rubbing the polyimide substrate. This direction manifested by scratches running diagonal through the micrographs of Figure 2 is uniform over large areas.

The high orientation is evident by the fiber diagram of the film (Figure 1). The fiber texture can be confirmed by the invariance of the diffraction diagram, when the film is tilted round the molecular axis. This direction in real space coincides with the direction toward the meridional reflection which is in reciprocal space, inferring orthogonality between the fiber axis and an hexagonal basal plane. The reflections on the equator exhibit the expected sequence for a unit cell of the hexagonal family. The observed reflections from several electron diffraction patterns are displayed in Table 1 together with the indexing in terms of a metrically hexagonal cell. They are not all seen in the current print of Figure 1.

Table 1. Observed and Calculated Reflections of a Thin Oriented PF2/6 Film from Electron Diffraction Data

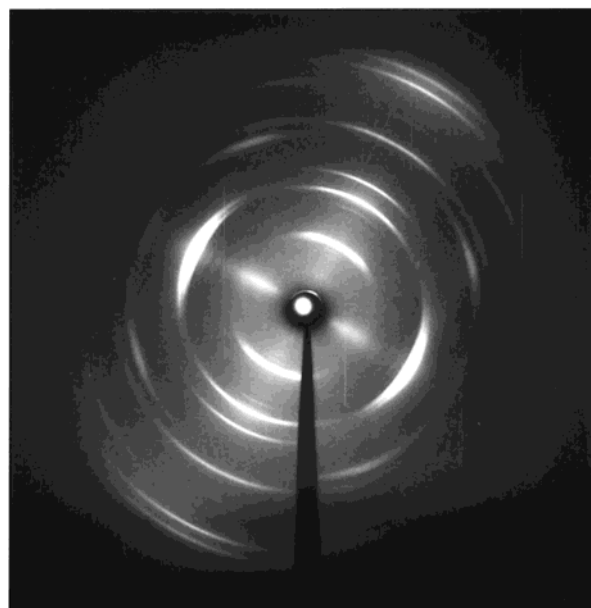
<i>hkl</i>	<i>d</i> _{obs} (Å)	<i>d</i> _{calc} (Å)
Equator		
10.0	14.46	14.43
11.0	8.34	8.33
20.0	7.20	7.22
21.0	5.43	5.46
30.0	4.81	4.81
22.0	4.18	4.17
31.0	4.00	4.00
40.0	3.60	3.61
32.0	3.31	3.31
First Layer Line		
10.1	13.60	13.59
20.1	7.10	7.10
21.1	5.40	5.41
31.1	3.96	3.98
Fifth Layer Line		
00.5	8.05	8.08
11.5	5.85	5.80
20.5	5.44	5.38
21.5	4.54	4.52
Sixth Layer Line		
10.6	6.15	6.10
21.6	4.26	4.24
Further Meridional Reflections		
00.10	observed	4.04
00.15	observed	2.69
00.20	observed	2.02

In Figure 1 the meridional reflection is arced owing to a narrow orientational distribution (dichroic ratio 15). On some of the electron diffraction patterns the meridional reflection has the tendency to degenerate into a continuous intensity distribution exhibiting a streak in the direction of the layer line, indicating that not all adjacent main chains are in register. The aliphatic side chains are disordered expressed by an halo with some sampling on the equator. An occasionally observed ring at a *d* value of about 14.5 Å is due to the polyimide substrate, as was proved by electron diffraction of a neat PI film prior to deposition of **PF2/6**.

The most prominent feature of the fiber diagram is the triple of reflections 10.1, 10.0, 10.1. The reflections with the indices *l* = ±1 define a first layer line; the innermost meridional reflection 00.1 is the 00.5 reflection. Also 00.10, 00.15 and 00.20 reflections are present in some of the fiber patterns.

The absence of meridional reflections with *l* ≠ 5*n* (*n* integer) is in favor of a 5/*q* - helix. For a discontinuous helix of the type *p*/*q* (*p* monomers on *q* turns) the intensity of a reflection is the square of the structure amplitude $F(R, \Psi, l/c) = \sum_n J_n(2\pi r_0 R) \exp[in(\Psi + \pi/2)]$ (*r*₀, radius of the helix; *R*, Ψ , cylindrical coordinates in reciprocal space). Together with the structure amplitude the selection rule *l* = *np* + *mq* is valid (*n*, *m* integers). *J_n* is the Bessel function of order *n*. For meridional reflections only the Bessel function of order 0 has a value ≠ 0 for the argument 0. All other Bessel functions are zero and the sum which controls the intensity is reduced to *J*₀(0).¹¹

Electron diffraction data are supported by X-ray diffraction results of a fiber drawn from the **PF** melt. When the fiber is annealed at 170 °C for the same duration of time (4 h) as the film the X-ray fiber pattern is in agreement with the electron diffraction data (Figure 3). However, another transient structure is responsible for additional very weak equatorial reflections which do not match the same unit cell. The *d* value

**Figure 3.** X-ray diffraction pattern of a fiber drawn from the same polymer and annealed subsequently at 170 °C for 4 h.

of the corresponding meridional reflection is slightly larger. After annealing for another 20 h at 170 °C the additional weak reflections disappear and the diffraction patterns of film and fiber coincide.

Preliminary data for the hexagonal unit cell of **PF2/6** in a thin film from 19 independent reflections are the parameters

$$a = b = 16.7 \text{ Å}, c = 40.4 \text{ Å}, \alpha = \beta = 90^\circ, \gamma = 120^\circ$$

With the molecular mass of a chemical repeating unit of 388.6 and *Z* = 3 a crystallographic density of $\rho = 0.996 \text{ g/cm}^3$ is calculated. The observation that the film sinks down in 2-propanol at room temperature ($\rho = 0.979 \text{ g/cm}^3$) determines a lower limit for the density. Although for the unit cell metrical hexagonal setting was selected, three chains running through the unit cell are not compatible with 6-fold rotational symmetry. The most probable choice in view of the limited number of data is therefore a unit cell of the trigonal crystal system with space group *P*3.

MO Calculations and Molecular Modeling. From accessible diffraction data alone, in particular from the lack of a second layer line, the prima facie choice of the *q*-parameter of the 5/*q* helix would be *q* = 1. However, MO calculations and molecular modeling performed to yield information on the geometry of the polyfluorene repeating unit, the chain conformation, and the *S*₀–*S*₁ transition energy are, together with the aspect of chain conjugation, more in favor of *q* = 2.

Figure 4 shows the molecular modeling result of 5/*q* helices of **PF** with *q* = 1, 2, based on RHF/6-31G calculations of bi- and terfluorene. (Since the corresponding helices for *q* = 4, 3 are only mirror images with respect to *q* = 1, 2, the handedness of the helices is neglected.) Details of these calculations will be published separately.¹² In short, a planar monomer unit with a total length of 8.39 Å was used. The bond angles between chemical repeat units used for the 5/1 and the 5/2 helix were 22.8 and 22.92°, with the torsional angles being 72 and 144° respectively. The projected monomer lengths were calculated to be 8.09 Å for *q* = 1 and 8.38 Å for *q* = 2, which are both in accordance with the

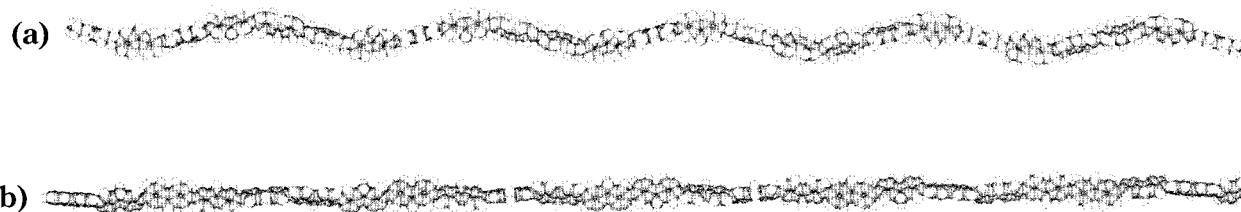


Figure 4. Molecular Modeling of oligo(25)-fluorene with 5/ q helix: (a) $q = 1$; (b) $q = 2$. Structures are based on RHF/6-31G calculations of bi- and terfluorene. Ethylhexyl side chains were replaced by hydrogen.

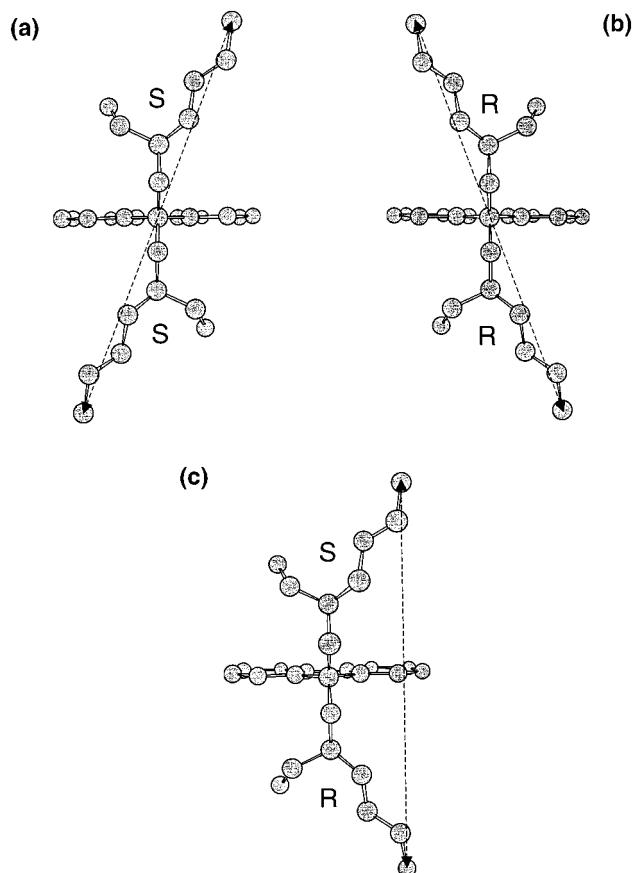


Figure 5. Optimized structures of a monomer of PF2/6 by RHF/6-31G calculations. Each ethylhexyl side chain of one monomer has (a) S - and S -, (b) R - and R -, and (c) S - and R -chirality. Sum of the length of side chains (including hydrogen, written as arrow) are 16.7 Å in the case of a and b, and 15.1 Å in the case of c.

length of the c -axis of the unit cell divided by 5. But, in contrast to the "helical" shape of the 5/1 helix, the 5/2 helix has a more "linear" shape, in which the orientation of the individual monomer units deviates only slightly from the main trajectory of the backbone.

Figure 5 shows the optimized structure of the monomer of PF2/6. The diameter of the monomer (perpendicular to the polymer chain and without restrictions owing to adjacent chains) is a function of the chirality of the side chain. It is estimated to be 16.7 Å for the monomers with S/S and R/R side chain chirality and 15.1 Å for the monomer with mixed chirality. Thus, the average diameter of the completely linear and ideal racemic chain would be 15.9 Å. These values need to be compared with the unit cell parameters a and b , which both are 16.7 Å. From this point of view the conformation of a 5/2 helix is favored compared to a 5/1 helix which is expected to widen the total diameter of the polymer chain significantly as shown in Figure 4a.

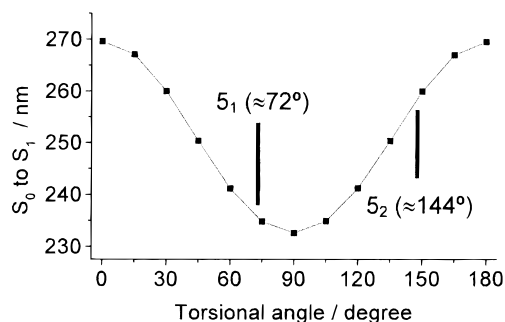


Figure 6. S_0 - S_1 electronic transition energy of fluorene-dimer as a function of the torsional angle. The transition energy was estimated by TD method, based on the optimized structures of bifluorene by RHF/6-31G calculations. Torsional angle of neighboring monomers are expected to be about 72° in the case of 5/1 helix, and about 144° in the case of 5/2 helix. The blue shift of the S_0 - S_1 electronic transition indicates the stronger distortion of conjugation in the case of a 5/1 helix.

Further support for the 5/2 helix structure comes from the torsional angle dependence of the electronic transition energy as shown in Figure 6. The torsional angle between neighboring monomers is about 72° in the case of a 5/1 helix, compared to about 144° in the case of a 5/2 helix. Therefore, the observed rather extended conjugation in PF2/6 as evidenced by the absorption and emission properties are in favor of a 5/2 helix.

The various configurational possibilities shown in Figure 5 classify PF2/6 as a copolymer, provided that the two enantiomeric forms of the side chain are randomly distributed along the polymer chain. Disorder in the side chain of rigid-rod polymers, suggested by the existence of the amorphous halo, is in favor of hexagonal packing of the macromolecules. Similar experience was made with the packing of isopentylcellulose as a function of the degree of substitution.¹³

Conclusion

The experimental data for PF2/6 chains in annealed samples support strongly packing in a trigonal lattice $a = b \neq c$, $\alpha = \beta = 90^\circ$, $\gamma = 120^\circ$. Both experimental and theoretical results suggest further a helical conformation of the polymer. In the present work, only investigations on a nonchiral PF (with a racemic mixture of the two enantiomeric forms of the branched side chains) were analyzed. Investigations of the chiroptical properties in absorption, photoluminescence and electroluminescence of nonchiral PF's did not reveal any significant optical activity, neither in solution nor in the solid state.¹⁴ In contrast, an enantiomeric excess induced strong optical activity of the polymer in thin solid films.¹⁵ As an example, annealed films of poly{[9,9-bis(3*S*,3,7-dimethyloctyl)]fluorene-*co*-[9,9-bis(ethylhexyl)]fluorene} with a fraction of the chiral-substituted units of 10% exhibit strong optical activity with an asymmetry factor g_{CD} in absorption of 0.04 (the asym-

metry factor for circular dichroism is defined as $g_{CD} = 2(\epsilon_L - \epsilon_R)/(\epsilon_L + \epsilon_R)$, with ϵ_L and ϵ_R being the extinction coefficients for left- and right-handed circularly polarized light, respectively). According to these results local variations of the side chain configuration are the reason for the type of helix with distinct handedness but side chains in random conformation.

Having a helix conformation in conjunction with the copolymer character due to the mixed chirality of the side chains, the nonchiral **PF2/6** can be considered as a "hairy-rod" molecule. These molecules have in common, that the wormlike backbone is surrounded by a cylindrical shell of disordered side chains. Those molecules are also known to orient well under shear, during Langmuir–Blodgett monolayer-transfer in the presence of a nonhomogeneous flow of the molecules at the air–water interface,¹⁶ in a strong magnetic field¹⁷ and on alignment layers.¹⁸ These good alignment properties are believed to stem from the low viscosity in the solid state, due to the flexible and disordered side chain shell around each individual polymer. As has been shown for the case of liquid crystalline main chain aromatic polyesters, the viscosity measured in dynamic rheology spectroscopy can be lower by several orders of magnitude in the nematic (hexagonal) phase compared to the layered (lamellar) phase, and might even be slightly lower than in the isotropic melt.¹⁹ The very large dichroic ratio of oriented **PF2/6** layers in absorption and the large polarization ratio in photoluminescence and electroluminescence can thus be well understood from the rather low viscosity of the metrically hexagonally packed cylindrically shaped polymers in conjunction with the almost linear structure of the proposed 5/2 helix.

Note that a second blue light-emitting liquid crystalline polymer, hexyl-dodecyl copoly(phenyleneethynylene),²⁰ did not show any appreciable alignment on polyimide alignment layers.^{3b} Experimental investigations as well as semiempirical calculations suggested that phenyleneethynylenes form sanidic lamellar LC phases, in which the rotation around the triple bond is restricted and a planar arrangement of the conjugated backbones with concomitant interchain π – π -stacking is observed.²¹ Those features are typically known for board-like polymers.²² **PFO** with linear side chains might just present a mixed-character, in which the bent monomer unit in conjunction with the rotational potential of the backbone favors a cylindrical helical conformation while the linear side chains induce a planar zigzag backbone conformation in the solid state under certain conditions. This mixed characteristics could well explain the lower degree of orientation of **PFO** on alignment layers compared to **PF2/6**.

Acknowledgment. We thank Dr. A. Yasuda, Dr. D. Lupo, and Prof. W. Knoll for fruitful discussions and

Mr. M. Steiert for technical support recording X-ray fiber diagrams. M. O. thanks the DAAD for the supporting his stay at the Max-Planck-Institute. This work was in part funded by Sony International (Europe).

References and Notes

- (1) (a) Grice, A. W.; Bradley, D. D. C.; Bernius, M. T.; Inbasekaran, M.; Wu, W. W.; Woo, E. P. *Appl. Phys. Lett.* **1998**, *73*, 629. (b) Kim, J. S. Friend, R. H.; Cacialli, F. *Appl. Phys. Lett.* **1999**, *74*, 3084. (c) Chen, J. P.; Klaerner, G.; Lee, J.-I.; Markiewicz, D.; Lee, V. Y.; Miller, R. D.; Scott, J. C. *Synth. Met.* **1999**, *107*, 129.
- (2) (a) Klaerner, G.; Davey, M. H.; Chen, W. D.; Scott, J. C.; Miller, R. D. *Adv. Mater.* **1998**, *10*, 993. (b) He, Y.; Gong, S.; Hattori, R.; Kanicki, J. *Appl. Phys. Lett.* **1999**, *74*, 2265.
- (3) (a) Grell, M.; Knoll, W.; Lupo, D.; Meisel, A.; Miteva, T.; Neher, D.; Nothofer, H.-G.; Scherf, U.; Yasuda, A. *Adv. Mater.* **1999**, *11*, 671. (b) Miteva, T.; Meisel, A.; Nothofer, H.-G.; Scherf, U.; Knoll, W.; Neher, D.; Grell, M.; Lupo, D.; Yasuda, A. *Proc. ICCEL 2, Sheffield 1999, Synth. Met.*, in press.
- (4) Miteva, T.; Meisel, A.; Nothofer, H.-G.; Scherf, U.; Knoll, W.; Neher, D.; Grell, M.; Lupo, D.; Yasuda, A. *Proc. SPIE* **1999**, *3797*, 231.
- (5) Grell, M.; Bradley, D. D. C.; Ungar, G.; Hill, J.; Whitehead, K. S. *Macromolecules*, **1999**, *32*, 5810.
- (6) Albrecht, C.; Lieser, G.; Wegner, G. *Prog. Colloid Polym. Sci.* **1993**, *92*, 111.
- (7) Wang, W.; Lieser, G.; Wegner, G. *Makromol. Chem.* **1993**, *94*, 1289.
- (8) Witteler, H.; Lieser, G.; Wegner, G.; Schulze, M. *Makromol. Chem., Rap. Commun.* **1993**, *14*, 471.
- (9) Wang, W.; Lieser, G.; Wegner, G. *Macromolecules* **1994**, *27*, 1027–1032.
- (10) Geis, M. W.; Flanders, D. C.; Smith, H. J. *Appl. Phys. Lett.* **1979**, *35*, 71.
- (11) Vainshtein, B. K. *Diffraction of x-rays by chain molecules*; Elsevier: Amsterdam, London, New York, **1966**.
- (12) Oda, M.; Lieser, G.; Nothofer, H.-G.; Scherf, U.; Neher, D. Manuscript in preparation.
- (13) Fakirov, C.; Lieser, G.; Wegner, G. *Macromol. Chem. Phys.* **1997**, *198*, 3407.
- (14) Oda, M.; Nothofer, H.-G.; Lieser, G.; Scherf, U.; Meskers, S. C. J.; Neher, D. *Adv. Mater.* **2000**, *12*, 362.
- (15) Oda, M.; Meskers, S. C. J.; Nothofer, H.-G.; Scherf, U.; Neher, D. Presented at the Proceedings of the ICCEL 2, Sheffield, U.K., 1999. *Synth. Met.*, in press.
- (16) Wegner, G.; Mathauer, K. *Mater. Res. Soc.* **1992**, *274*, 767. Wegner, G. *Mol. Cryst. Liq. Cryst.* **1993**, *235*, 1.
- (17) Alu-Adip, Z.; Davison, K.; Nooshin, H.; Tredgold, R. H. *Thin Solid Films* **1991**, *201*, 187.
- (18) Witteler, H. Ph.D. Thesis, University of Mainz, 1994.
- (19) Damman, S. B.; Mercx, F. P. M.; Kootwijk-Damman, C. M. *Polymer* **1993**, *9*, 189.
- (20) Kloppenburg, L.; Song, D.; Bunz, U. H. F. *J. Am. Chem. Soc.* **1998**, *120*, 7973.
- (21) (a) Bunz, U. H. F.; Enkelmann, V.; Kloppenburg, L.; Jones, D.; Shimizu, K. D.; Claridge, J. B.; zur Loye, H.-C.; Lieser, G. *Chem. Mater.* **1999**, *11*, 1416. (b) Miteva, T.; Palmer, L.; Kloppenburg, L.; Neher, D.; Bunz, U. H. F. *Macromolecules* **2000**, *33*, 652.
- (22) Ballauff, M. *Angew. Chemie., Int. Ed. Engl.* **1989**, *28*, 253. Neher, D. *Adv. Mater.* **1995**, *7*, 691.

MA9921652